Supporting Information

Weerakkody et al. 10.1073/pnas.1303708110

SI Materials and Methods

Conjugation of pH (Low) Insertion Peptide Variants with Fluorescent Dyes. The pH (low) insertion peptide (pHLIP) variants were prepared by solid-phase peptide synthesis using Fmoc chemistry and purified by reverse phase chromatography at the W. M. Keck Foundation Biotechnology Resource Laboratory at Yale University. For cell and in vivo studies, variants were conjugated with AlexaFluor750-C_5-maleimide, tetramethylrhodamine (Rho)-5-maleimide, single isomer, or boron-dypyrromethene (BODIPY)-tetramethylrhodamine (TMR)-C_5-maleimide (Invitrogen).

The lyophilized powder of a peptide was dissolved in a solution containing 3 M urea, and the peptide solution was transferred to buffer using a G-10 size-exclusion spin column or was dissolved directly in phosphate buffer at pH 8 for biophysical studies. The concentrations of the peptides were determined by absorbance [for variant (Var) 0–2 and Var14–16: ε_{280} = 13,940 $M^{-1}\cdot cm^{-1}$; and for Var3–13, K (Lys)-Var3, and K (Lys)-Var7: ε_{280} = 12,660 $M^{-1}\cdot cm^{-1}$].

For studies on cultured cells and animals, each pHLIP variant was conjugated with AlexaFluor750 C_5-maleimide (catalog no. A30459; Invitrogen) and Var3, Var7, K-Var3, and K-Var7 were conjugated with Rho-5-maleimide, single isomer (catalog no. T6027; Invitrogen) or BODIPY-TMR C_5-maleimide (catalog no. B30466; Invitrogen) in dimethylformamide or DMSO at a ratio of 1:1.1 of dye/peptide and incubated at room temperature for about 6 h and then at 4 °C until the conjugation reaction was completed. The reaction progress was monitored by reverse phase HPLC. The purity of products was assessed by analytical HPLC, and peak identity was confirmed by surface-enhanced laser desorption/ionization TOF MS.

Liposome Preparation. Large unilamellar vesicles (LUVs) were prepared by extrusion. 1-Palmitoyl-2-oleoyl-sn-glycero-3-phosphocholine (POPC; Avanti Polar Lipids, Inc.) dissolved in chloroform at a concentration of 1 mg/mL was desolvated on a rotary evaporator and dried under high vacuum for several hours. The phospholipid film was then rehydrated in 100 mM phosphate buffer (pH 8.0), vortexed for 2 h, and repeatedly extruded through membranes with a 100- or 50-nm pore size to obtain LUVs.

Steady-State Fluorescence and CD Measurements. Peptide intrinsic fluorescence and CD measurements were carried out on a PC1 ISS spectrofluorometer (ISS, Inc.) and a MOS-450 spectrometer (Biologic, Inc.), respectively, under temperature control at 25 °C. Peptide fluorescence spectra were recorded with the spectral widths of excitation and emission slits set at 4 and 2 nm, respectively, using an excitation wavelength of 295 or 280 nm. The concentrations of the peptides and POPC liposomes were 7 μM and 1.5 mM, respectively.

Oriented CD Measurements. Oriented CD was measured from supported bilayers deposited on a stack of quartz slides with special polish for far UV measurements, with spacers of 0.2-mm thickness on one side of each slide (Starna). Quartz slides were cleaned by sonication for 10 min in cuvette cleaner solution (5% Contrad in water; Decon Labs), 2-propanol, acetone, and 2-propanol again; they were then rinsed with deionized water. The slides were immersed in a mixture of concentrated sulfuric acid and hydrogen peroxide (3:1 ratio) for 5–10 min to remove any remaining organic material completely from the slides. Slides were then thoroughly rinsed with and stored in deionized water (Milli-Q purified water kept at 25 °C). A POPC lipid monolayer was deposited on the clean quartz substrate by the Langmuir–Blodgett (LB) method using a KSV minitrough (KSV Instruments). For the LB deposition, a POPC lipid solution in chloroform was spread on the subphase and allowed to evaporate chloroform for about 30 min, followed by monolayer compression to 32 mN/m. An initial layer was deposited by retrieving the slide from the subphase at a rate of 15 mm/min. The second layer of the bilayer was created by fusion. For this step, the monolayer on the slide was incubated with a solution of POPC vesicles (50 nm in diameter obtained by extrusion) mixed with the peptide solution at pH 4 (0.5 mM POPC and 10 μM peptide). The fusion occurred during 6 h of incubation at 100% humidity. Excess vesicles were then carefully removed, and the slides were stacked to make a pile filled with the peptide solution (5 μM) at pH 4. Bilayers with the peptide solution were allowed an additional 6 h of equilibration. Measurements were taken at three steps during the process: when the monolayers were incubated with the excess of liposomes, soon after spaces between slides were filled with the peptide solution, and 6 h after the second measurement. Fourteen slides (28 bilayers) were assembled, and oriented CD spectra were recorded on a MOS-450 spectrometer with 2 s of sampling time. Control measurements were carried out on the peptide between slides with and without supported bilayers and in the presence of an excess of POPC liposomes.

Titration Experiments. Samples containing 5 μM peptides and varying concentrations of lipids were prepared using an electronic repeater pipette (Eppendorf). Different pHs were used for peptides with different pK_as of insertion; the pH of the solution was 1 pH unit below the apparent pK value for each peptide. The samples at high and low pHs were allowed to equilibrate at 4 °C overnight or for 2 h, respectively, before the measurements. The peptide intrinsic fluorescence spectra were measured using 280 nm excitation at 25 °C with the emission polarizer set at 90° to reduce the contribution of scattered light. A series of POPC blanks with the same concentrations of lipids at pH 8 were measured with the same instrument settings and were subtracted from the corresponding fluorescence spectra of peptides in the presence of POPC. The areas under the emission spectra were calculated, and the values were normalized to the first point (the emission of the peptide in the absence of POPC). The titration data were fitted by the peptide-membrane partition model to calculate the mole-fraction partition coefficient, K:

$$F = F_0 + \cdot F \frac{K \cdot C_{lip}}{W + K \cdot C_{lip}},$$

where F_0 and ΔF are the fluorescence intensity at the beginning and fluorescence increase as a result of the titration ($F_0 = 1$ in our case), respectively; C_{lipids} is the concentration of lipids; and W is the molar concentration of water (55.3 M). Nonlinear least squares curve fitting procedures using the Levenberg–Marquardt algorithm were implemented in Origin 8.5.0 SR1 (OriginLab, Corp.). The Gibbs free energy (ΔG) was calculated according to the equation:

$$\Delta G = -RT \cdot ln(K),$$

where R is the gas constant and T is the temperature in Kelvin.

pH Dependence. The pH-dependent partitioning of the peptides into lipid bilayers was investigated by the shift of the position of the peptide intrinsic fluorescence spectral maximum for the pHLIP variants induced by a drop of pH from pH 8 to pH 3 by means of the addition of HCl in the presence of POPC liposomes.

Peptide (3 μM) was incubated overnight with 100 nm of POPC liposomes (2 mM), and the pH was decreased by the addition of aliquots of 4, 2, 1, and 0.1 M HCl. The resulting pHs were measured using a microelectrode probe (Orion Ross Micro pH electrode; Thermo Electron Corporation). Fluorescence spectra were recorded at each pH value. The spectra were analyzed by decomposition algorithms using an online protein fluorescence and structural toolkit (PFAST) to obtain spectral maxima (λ_{max}). Finally, the positions of the fluorescence spectral maxima (λ_{max}) of the single-component solutions were plotted vs. pH, and the Henderson–Hasselbalch equation was used to fit the data: $\lambda_{max} = \lambda^2_{max} + \frac{(\lambda^1_{max} - \lambda^2_{max})}{1+10^{n\cdot(\mathrm{pH}-pKa)}}$, where $\lambda^1{}_{max}$ and $\lambda^2{}_{max}$ are the beginning and end of the transition, n is the cooperativity parameter, and pKa is the midpoint of the transition.

Peptide intrinsic fluorescence changes are used to follow the insertion as a function of pH (transition from state II to state III as the pH is lowered). Decomposition of the fluorescence spectra measured at various pHs gives the positions of the maxima, and the single-component solutions are shown (Fig. 2). The Henderson–Hasselbalch equation with cooperativity was used to fit the experimental points, and the fitting curves and 95% confidence intervals are shown by the red and blue lines, respectively. Each graph notes the apparent pK of the peptide's insertion into the membrane obtained from the fitting of the experimental data. The pK_a of Var0 (WT-pHLIP) is 6.0. The pK_a values obtained by fitting of the experimental data by the Henderson–Hasselbalch equation with a fixed cooperativity parameter ($n = 1$) are very similar to the data shown in the figure: Var1 = 6.14, Var2 = 5.59, Var3 = 5.09, Var4 = 5.32, Var5 = 4.84, Var6 = 5.06, Var7 = 5.51, Var8 = 5.75, Var9 = 5.59, Var10 = 4.92, Var11 = 5.52, Var12 = 4.52, Var13 = 5.16, Var14 = 5.69, Var15 = 5.59, and Var16 = 5.63. It is assumed that there is a linear relation between the position of the maximum and the contribution of state II or state III (state I is the peptide in solution at pH 8, state II is the peptide in the presence of POPC liposomes at pH 8, and state III is the result of folding and insertion of the peptide with POPC when the pH is dropped from pH 8 to pH 3.6 by the addition of an aliquot of HCl). However, due to the fact that the quantum yields in states II and III are slightly different, there was a slight nonlinearity; thus, we completed the analysis by estimating the contributions of the states for Var7-pHLIP and found that the apparent pK shifts no more than on 0.05 pH units toward lower pHs. Because this shift is less than the experimental error, we present the pK_a values for transitions from state II to state III based on the analysis of the positions of spectral maxima.

Stopped-Flow Fluorescence Measurements. Stopped-flow fluorescence measurements were carried out on an SFM-300 mixing apparatus connected to a MOS-450 spectrometer under temperature control. All solutions were degassed for several minutes under vacuum before loading into the syringes to minimize air bubbles. pHLIP variants (7 μM) were preincubated with POPC (1.5 mM) at pH 8.0 to reach binding equilibrium, and insertion was induced by fast mixing (5-ms dead time) of equal volumes of pHLIP-POPC variants at pH 8.0 and appropriately diluted HCl to obtain a drop of pH from pH 8 to the desired value. Each kinetic curve was recorded several times (~10 times) and then averaged, excluding the first two to three shots.

Cell Lines. Human cervix adenocarcinoma (HeLa) and human lung carcinoma (A549) cells were acquired from the American Type Culture Collection. Human lung carcinoma and human cervix adenocarcinoma cells with stable expression of GFP, A549-GFP, and HeLa-GFP, respectively, were acquired from Cell Biolabs, Inc. Cells were authenticated, stored according to the supplier's instructions, and used within 3 mo after frozen aliquot resuscitations. Cells were cultured in DMEM supplemented with 10% FBS and 10 μg/mL ciprofloxacin in a humidified atmosphere of 5% CO_2 and 95% air at 37 °C. The pH 5.9 medium was prepared by mixing 13.3 g of dry DMEM in 1 L of deionized water. Human cervical (HCvEpC), human mammary (HMEpC), and human bronchial (HBEpC) epithelial cells were acquired from Cell Applications, Inc. Cells were authenticated, stored according to the supplier's instructions, and used within 2 mo. HCvEpCs, HMEpCs, and HBEpCs were cultured in cervical, mammary, and bronchial epithelial cell growth medium, respectively, provided by Cell Applications, Inc.

Fluorescence Microscopy. HeLa-GFP and A549-GFP cells were grown in 35-mm dishes with 14-mm glass-bottomed windows coated with poly-D-lysine or collagen. Cells were washed with DMEM not containing FBS (pH 5.9 or pH 7.4) and then incubated with 2 μM Rho- or BODIPY-labeled Var3, K-Var3, Var7, or K-Var7 peptides at pH 5.9 or pH 7.4. After 30 min of incubation, cells were washed four to five times. Fluorescent images were acquired with a Retiga CCD camera (Qimaging) mounted to an inverted Olympus IX71 microscope (Olympus America, Inc.).

Quantification of Cellular Uptake. For quantification of cellular uptake of BODIPY-labeled Var3 and Var7 at pH 7.4 and pH 5.9, we used A549-GFP cells in suspension. Fluorescently labeled peptides (2 μM) were incubated with cells in DMEM media at pH 7.4 and pH 5.9 for 30 min at 37 °C and 5% (vol/vol) CO_2 and 95% (vol/vol) air. Then, cells were pelleted by centrifugation ($600 \times g$ for 4 min) at room temperature, the supernatant was removed, the pellet was washed three times with the same media and resuspended in 50 μL of media, and the cell suspension solution was placed into cell counting chambers. The phase-contrast GFP and BODIPY fluorescent signals were measured and analyzed using the ImagePro Plus program (Media Cybernetics, Inc.).

Cytotoxicity Assay. HeLa cells, A549 cells, HCvEpCs, HMEpCs, or HMEpCs were loaded in the wells of 96-well plates (~5,000 cells per well) and incubated overnight. The increasing amounts of pHLIP variants (1, 2, 4, and 8 μM) were added to HCvEpCs, HMEpCs, or HMEpCs, or growth medium was replaced with the medium without FBS containing increasing amounts of pHLIP, and after 3 h of incubation, an equal volume of the medium containing 20% of FBS was added in the case of HeLa and A549 cells. After 24, 48, and 72 h of incubation, a colorimetric reagent (CellTiter 96 AQ_{ueous} One Solution Assay; Promega) was added for 1 h, followed by measuring absorbance at 490 nm to assess cell viability. All samples were prepared in triplicate. None of the tested pHLIP variants showed any cytotoxic effect.

Animal Studies. Athymic female nude mice ranging in age from 4 to 6 wk and weighing from 15 to 18 g were obtained from Harlan Laboratories. In total, 266 mice were used in the experiments, and the number of mice used to study each pHLIP variant can be found in Tables S2–S5. Mouse tumors were established by s.c. injection of HeLa-GFP or A549-GFP cells (10^6 cells per 0.1 mL per flank) in the right flank of each mouse. When tumors reached 5–6 mm in diameter, tail vein injections of 100 μL of Alexa750-pHLIPs (40 μM) were performed. Animals were imaged at 4 and 24 h postinjection on an FX Kodak in vivo image station under gas anesthesia with supplemental heat provided to maintain core body temperature. Animals were euthanized at 4 or 24 h, and necropsy was performed immediately after euthanization. Tumors and major organs were collected for further imaging. The tumor/organ ratio was calculated according to the equation:

$$\frac{\text{Tumor}}{\text{Organ}} = \frac{F_{tumor} - F_{backg}}{F_{organ} - F_{backg}},$$

where F_{tumor}, F_{organ}, and F_{backg} are the mean fluorescence intensities of tumor, organ, and background signal, respectively. The contrast-to-noise ratio (*CNR*) was calculated according to the equation:

$$CNR = \frac{F_{tumor} - F_{backg}}{SD_{backg}},$$

where SD_{backg} is the SD of the background signal. Fluorescence intensity was obtained from image analysis using Kodak software. Statistical analysis of the data was performed using the Statistica 5.0 package (StatSoft, Inc.). The probability level was computed based on the two-tailed test. All animal studies were conducted according to an approved University of Rhode Island animal protocol (AN07-01-015), in compliance with the principles and procedures outlined in the National Institutes of Health Guide for the Care and Use of Animals.

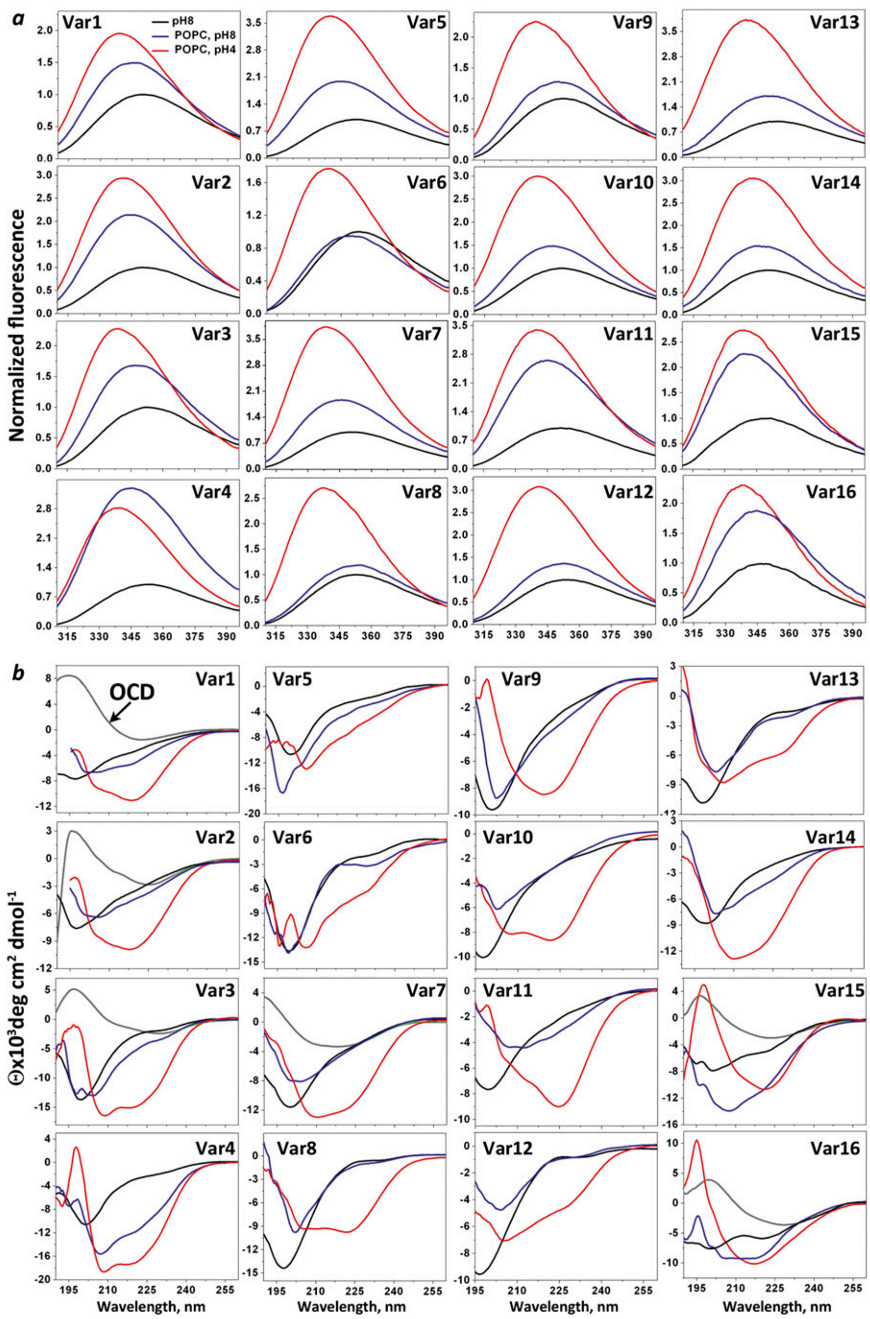

Fig. S1. Three states of pHLIP variants. The pHLIP variants were studied for the presence of the three basic states of pHLIP: state I is the peptide in solution at pH 8 (black lines), state II is the peptide in the presence of POPC liposomes at pH 8 (blue lines), and state III is the folding and insertion of the peptide with POPC when the pH is dropped from pH 8 to pH 3.6 by the addition of an aliquot of HCl (red lines). The states are monitored by changes of the steady-state tryptophan fluorescence at $\lambda_{ex} = 295$ nm (*A*) and CD (*B*) spectroscopic signals. The concentrations of the peptides and POPC were 7 μM and 1.5 mM, respectively. State I: In aqueous solution at pH 8 and in the absence of lipids, all variants except Var16 (and Var1 to some degree) have long wavelength emission maxima and are largely unstructured. Further, the addition of several Asp residues to the N terminus (Var15) significantly increases peptide solubility compared with a similar sequence investigated previously, which has no Asp at the N terminus. State II: When liposomes are added to the solution, the majority of the peptide is bound at the surface of the membrane, as observed by a shift of the emission maxima to shorter wavelengths and an increase of fluorescence intensity. In the cases of Var4, Var15, and Var16, partial formation of an α-helical structure is seen, whereas all other pHLIP variants are predominantly unstructured. State III: When the pH is lowered, we observe formation of a helical structure and further propagation of tryptophan residues into the membrane, reflected by a further blue shift of the fluorescence maximum and a further increase of intensity relative to state II, with the single exception of Var4. There is some variation in the positions of the maxima and the increases of intensity in states II and III for different peptides, which could result from differences in the positioning of the tryptophan fluorophores as a result of the sequence changes. The strength of helical signal is smallest for Var12 and Var13 in state III, which most probably have less stable transmembane configurations given their lengths. For the variants 1, 2, 3, 7, 15, and 16, the oriented CD (OCD) signal was measured at low pH on supported bilayers (green curves). In each case, the helical orientation was found to be TM.

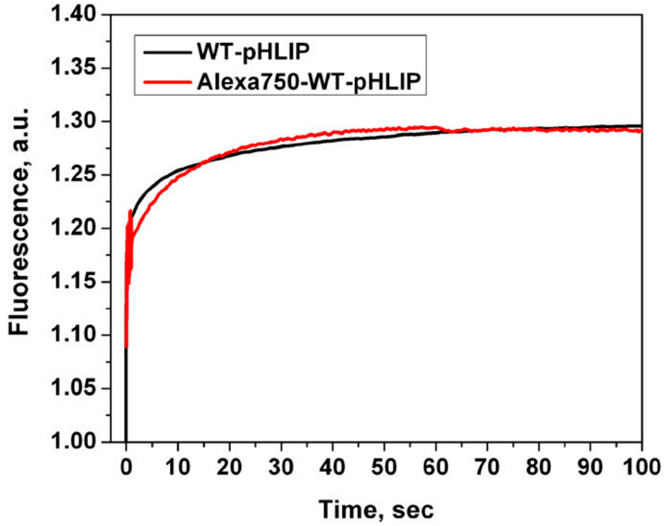

Fig. S2. Comparison of the kinetics of WT-pHLIP and Alexa750-WT-pHLIP insertion into the membrane. The changes of tryptophan fluorescence signal of Alexa750-WT-pHLIP in the presence of POPC liposome as a result of a pH drop from pH 8 to pH4–5 were recorded in a stopped-flow apparatus, multiplied by (−1), normalized, and compared with the kinetics of insertion of nonlabeled WT. a.u., arbitrary units.

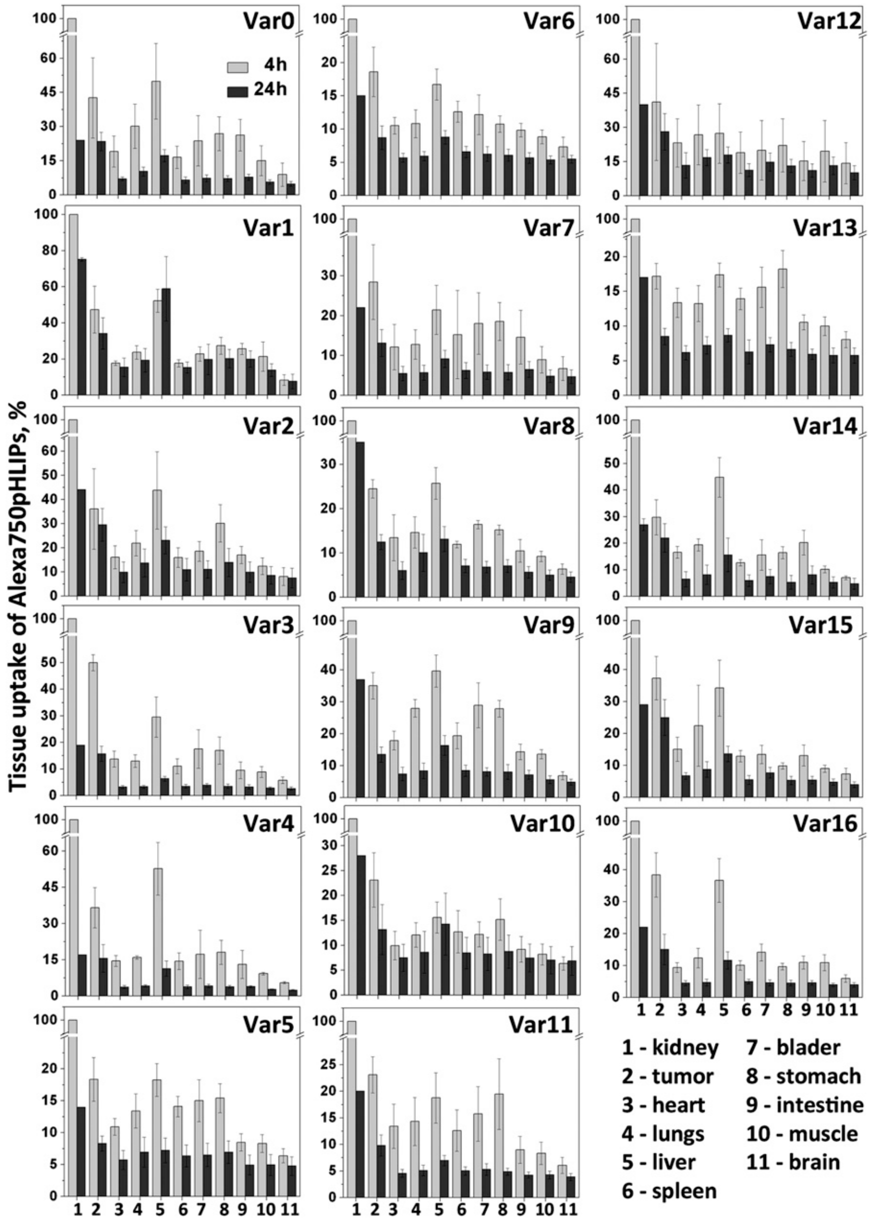

Fig. S3. Distribution of Alexa750-pHLIP in organs and tumors. Normalized mean near infrared fluorescence values of tumor and organs at 4 and 24 h after construct administration are shown (the signals in kidney at 4 h are taken as 100%). The nonnormalized values of fluorescence are given in Tables S2 and S3.

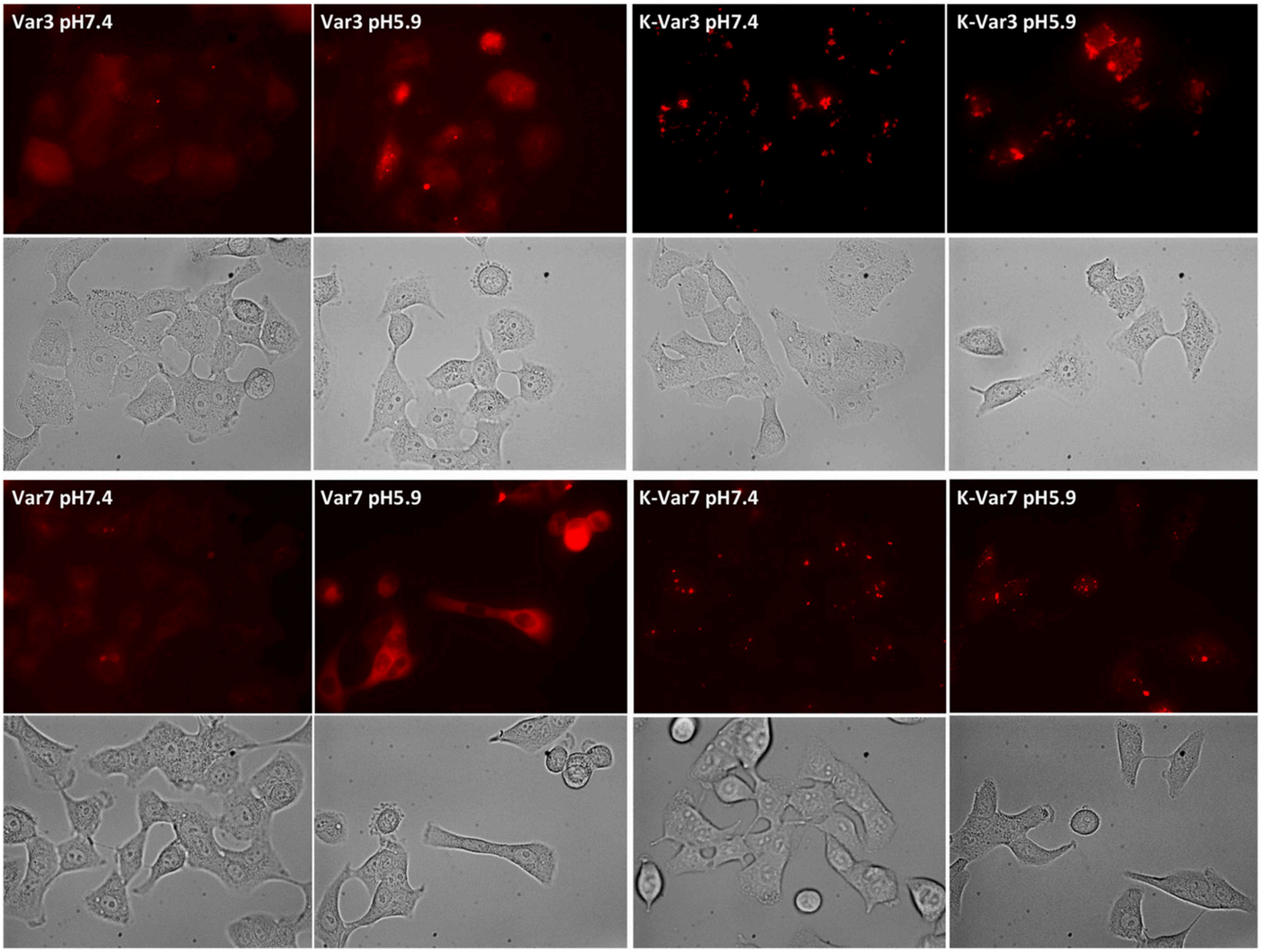

Fig. S4. Cellular uptake of BODIPY-labeled Var3, Var7, K-Var3, and K-Var7. Fluorescence and phase-contrast images of cells treated with fluorescence peptides at pH 7.4 and pH 5.9 for 30 min and washed four to five times with the same media are shown. Cell experiments were also carried out with Alexa750-labeled Var3, Var7, K-Var3, and K-Var7. Despite the fact that the signal was low (due to the low near infrared sensitivity of the Retiga CCD camera), the distribution of the signal in cells was the same as in the case of Rho- and BODIPY-labeled peptides. All images were obtained under an inverted optical microscope with a 60× objective.

Table S1. Three states of each pHLIP variant

Parameters	Name	State I	State II	State III
	Var1	349	345	339
		1	1.47	1.81
		−2.42	−3.85	−9.46
λ_{max}	Var2	350	345	342
S		1	2.08	2.76
$\theta_{225} \times 10^3$		−2.74	−3.76	−8.64
	Var3	353	347	338
		1	1.66	2.08
		−2.07	−3.94	−13.49
	Var4	353	340	345
		1	2.66	3.32
		−2.32	−10.14	−15.28
	Var5	351	355	340
		1	2.05	3.52
		−2.20	−3.38	−6.25
	Var6	353	350	339
		1	0.96	1.64
		−2.12	−2.89	−6.95
	Var7	352	345	340
		1	1.74	3.08
		−2.64	−4.12	−8.82
	Var8	353	353	337
		1	1.19	2.48
		−0.89	−1.22	−9.43
	Var9	353	350	339
		1	1.28	2.10
		−2.39	−3.20	−7.90
	Var10	350	347	340
		1	1.47	2.86
		−2.40	−2.46	−8.40
	Var11	351	345	340
		1	2.60	3.20
		−2.14	−3.08	−9.02
	Var12	353	352	341
		1	1.36	2.90
		−0.82	−0.96	−4.80
	Var13	355	349	340
		1	1.72	3.61
		−1.76	−2.28	−6.14
	Var14	351	346	344
		1	1.54	2.94
		−2.00	−3.79	−9.91
	Var15	351	339	339
		1	2.14	2.52
		−4.30	−8.94	−10.08
	Var16	346	345	339
		1	1.89	2.14
		−5.41	−7.03	−8.57

The spectral parameters of the pHLIP variants in states I, II, and III are presented. The parameters were obtained from analysis of the fluorescence and CD spectra shown in Fig. 1. The maximum position of the fluorescence spectrum, λ_{max}, is expressed in nanometers; S is the normalized area under the spectra (normalization was done on the area under the spectrum in state I); and $\theta_{225} \times 10^3$ (degrees per $cm^2 \cdot dmol^{-1}$) is the molar ellipticity at 225 nm.

Table S2. Mean near infrared fluorescence with SD calculated for each organ collected at 4 h after Alexa750-pHLIP variant administration

Organ	Var0-WT $n = 9$	Var1 $n = 6$	Var2 $n = 5$	Var3 $n = 7$	Var4 $n = 4$	Var5 $n = 5$	Var6 $n = 5$	Var7 $n = 16$	Var8 $n = 5$	Var9 $n = 5$	Var10 $n = 6$	Var11 $n = 6$	Var12 $n = 7$	Var13-1E $n = 6$	Var14 $n = 5$	Var15-2N $n = 5$	Var16-2P $n = 6$
Kidney	3,630.6 ± 485.6	4,324.0 ± 444.6	3,456.3 ± 585.4	6,125.6 ± 1004.1	6,755.6 ± 698.7	3,097.0 ± 528.3	2,536.1 ± 297.2	3,583.3 ± 47.9	3,729.2 ± 749.0	3,367.9 ± 667.6	3,575.0 ± 540.4	4,164.3 ± 833.5	2,004.5 ± 527.7	2,653.7 ± 357.1	4,162.9 ± 210.7	5,657.0 ± 843.8	3,733.0 ± 582.9
Tumor	1,373.8 ± 334.5	1,812.4 ± 819.0	1,145.3 ± 737.5	3,054.9 ± 726.2	2,439.3 ± 443.2	559.4 ± 95.6	461.6 ± 71.6	970.1 ± 449.1	910.6 ± 180.1	1,169.4 ± 297.9	819.9 ± 306.7	981.0 ± 357.9	614.5 ± 186.7	459.0 ± 99.3	1,245.0 ± 308.7	2,075.8 ± 252.2	1,407.0 ± 142.1
Heart	621.4 ± 152.3	752.9 ± 398.4	554.6 ± 421.2	855.0 ± 331.6	980.5 ± 187.3	334.0 ± 43.4	262.2 ± 29.5	351.1 ± 81.0	515.0 ± 284.4	613.4 ± 250.6	341.5 ± 87.7	532.3 ± 104.5	368.7 ± 100.4	351.7 ± 61.5	691.0 ± 104.7	837.6 ± 188.0	342.7 ± 28.9
Lungs	1,003.6 ± 297.5	1,016.6 ± 567.7	761.1 ± 506.8	803.1 ± 256.2	1,077.3 ± 84.2	405.4 ± 34.5	266.4 ± 23.7	413.3 ± 135.6	526.0 ± 62.2	958.0 ± 367.2	412.8 ± 42.4	560.2 ± 42.2	423.8 ± 122.0	349.7 ± 78.9	808.2 ± 116.3	1,190.8 ± 419.3	451.0 ± 85.2
Liver	1,651.4 ± 470.2	2,309.7 ± 1,457.0	1,432.4 ± 950.8	1,829.6 ± 741.6	3,615.3 ± 1,099.4	561.2 ± 103.0	414.8 ± 31.8	695.1 ± 244.2	938.2 ± 79.2	1,309.2 ± 255.3	539.0 ± 114.3	744.2 ± 57.1	435.9 ± 139.0	457.2 ± 46.8	1,863.0 ± 312.6	1,888.8 ± 303.1	1,344.0 ± 153.2
Spleen	546.4 ± 131.4	757.5 ± 445.0	539.3 ± 372.3	675.6 ± 244.6	987.3 ± 320.8	432.2 ± 63.0	316.0 ± 50.6	479.3 ± 310.6	443.8 ± 86.8	629.2 ± 96.1	423.4 ± 29.3	495.7 ± 46.5	295.7 ± 75.5	365.2 ± 20.4	527.8 ± 64.6	717.4 ± 61.9	370.7 ± 24.0
Bladder	825.4 ± 495.8	1,030.5 ± 646.3	665.3 ± 486.4	1,104.6 ± 628.7	1,198.8 ± 719.3	452.4 ± 47.6	298.6 ± 38.3	554.4 ± 243.4	608.8 ± 113.3	942.0 ± 204.0	420.0 ± 77.3	623.0 ± 145.3	287.2 ± 51.5	414.7 ± 102.9	648.6 ± 235.5	743.6 ± 59.8	525.7 ± 121.2
Stomach	909.2 ± 277.1	1,249.6 ± 783.1	1,092.0 ± 793.5	1,029.6 ± 355.0	1,239.8 ± 438.8	470.8 ± 71.7	268.6 ± 31.2	605.6 ± 205.6	563.4 ± 93.3	934.2 ± 251.3	513.1 ± 70.2	763.0 ± 107.8	341.2 ± 84.6	483.3 ± 96.1	685.6 ± 101.3	556.6 ± 94.6	361.2 ± 61.5
Intestine	884.2 ± 260.5	1,116.4 ± 646.0	590.9 ± 347.0	574.3 ± 221.9	888.5 ± 442.9	257.6 ± 23.0	246.4 ± 35.0	437.8 ± 109.2	380.6 ± 87.7	471.8 ± 98.9	321.6 ± 109.2	353.3 ± 14.7	227.5 ± 59.0	277.8 ± 31.1	839.8 ± 196.9	720.4 ± 52.9	403.3 ± 67.3
Muscle	476.8 ± 110.1	766.5 ± 285.3	413.7 ± 248.9	541.9 ± 180.3	629.8 ± 97.9	250.6 ± 17.9	220.8 ± 30.0	277.8 ± 67.2	339.0 ± 50.7	450.8 ± 97.8	281.5 ± 70.0	330.2 ± 22.2	270.8 ± 30.7	261.8 ± 24.4	421.4 ± 35.8	500.6 ± 37.1	396.0 ± 37.8
Brain	270.1 ± 46.3	303.1 ± 113.3	233.5 ± 72.9	350.6 ± 95.6	372.3 ± 13.9	193.2 ± 13.5	180.2 ± 18.7	206.3 ± 36.0	230.2 ± 18.4	222.0 ± 16.7	217.4 ± 26.4	241.5 ± 24.7	207.0 ± 33.0	211.0 ± 13.5	290.6 ± 27.2	405.0 ± 65.5	216.7 ± 14.9

The mean fluorescence values of organs were normalized to the signal in kidney for each mouse and then averaged for each variant; they are presented in Fig. S3. *n*, number of animals.

Table S3. Mean near infrared fluorescence with SD calculated for each organ collected at 24 h after administration of Alexa750-pHLIP variants

Organ	Var0-WT $n = 9$	Var1 $n = 4$	Var2 $n = 9$	Var3 $n = 7$	Var4 $n = 3$	Var5 $n = 5$	Var6 $n = 5$	Var7 $n = 17$	Var8 $n = 5$	Var9 $n = 5$	Var10 $n = 5$	Var11 $n = 4$	Var12 $n = 6$	Var13 $n = 3$	Var14 $n = 5$	Var15-2N $n = 5$	Var16-2P $n = 6$
Kidney	854.4 ± 186.9	3,349.5 ± 2,262.1	1,525.2 ± 472.4	1,141.8 ± 416.7	1,151.4 ± 262.4	431.0 ± 121.5	380.5 ± 46.0	785.3 ± 200.9	1,287.1 ± 307.6	1,242.2 ± 280.6	1,013.5 ± 104.4	828.6 ± 129.1	469.8 ± 72.1	444.9 ± 88.9	1,157.4 ± 147.5	1,618.9 ± 283.3	819.3 ± 124.1
Tumor	818.8 ± 157.4	1,366.1 ± 776.7	881.4 ± 560.6	950.9 ± 434.1	1,106.3 ± 651.1	252.2 ± 67.6	218.6 ± 40.8	453.1 ± 173.2	441.6 ± 102.0	441.2 ± 53.9	345.1 ± 140.2	400.3 ± 61.0	323.7 ± 93.8	218.3 ± 15.1	867.4 ± 286.1	1,416.0 ± 468.6	575.5 ± 231.1
Heart	248.5 ± 33.3	580.9 ± 280.2	240.3 ± 94.3	186.0 ± 31.3	255.0 ± 75.1	166.0 ± 16.0	142.8 ± 4.9	173.3 ± 20.3	201.8 ± 19.8	247.0 ± 92.6	196.8 ± 79.3	186.3 ± 10.6	202.7 ± 23.7	157.7 ± 6.7	230.8 ± 23.7	370.8 ± 52.3	164.2 ± 20.1
Lungs	355.7 ± 38.8	758.3 ± 422.8	351.9 ± 190.9	190.4 ± 31.8	287.7 ± 93.6	198.6 ± 15.3	148.8 ± 8.4	181.6 ± 24.2	330.2 ± 76.0	270.6 ± 58.6	198.4 ± 17.3	207.3 ± 8.7	221.1 ± 30.7	184.7 ± 8.3	285.4 ± 67.0	473.2 ± 68.9	171.3 ± 29.5
Liver	602.2 ± 104.4	2,211.1 ± 973.9	660.8 ± 427.5	366.3 ± 72.0	737.3 ± 90.4	209.0 ± 18.2	220.2 ± 5.7	299.8 ± 51.7	455.6 ± 76.9	536.0 ± 101.4	338.3 ± 47.5	285.5 ± 12.4	252.3 ± 32.9	224.0 ± 21.9	567.2 ± 130.6	742.8 ± 50.2	421.5 ± 52.7
Spleen	226.1 ± 13.0	626.3 ± 368.0	285.3 ± 170.8	199.0 ± 25.5	249.3 ± 30.7	184.0 ± 14.5	164.0 ± 69.0	200.1 ± 22.6	244.8 ± 39.1	273.6 ± 7.3	217.0 ± 71.8	204.3 ± 15.1	165.8 ± 98.0	158.3 ± 10.4	221.6 ± 40.7	295.8 ± 34.5	183.3 ± 13.9
Bladder	250.2 ± 27.5	861.6 ± 743.0	301.3 ± 183.5	221.6 ± 33.2	282.3 ± 72.8	188.0 ± 10.8	156.0 ± 10.8	187.2 ± 23.5	236.8 ± 37.7	264.2 ± 30.6	207.4 ± 60.2	214.3 ± 18.2	242.7 ± 26.6	188.0 ± 16.6	274.6 ± 36.8	417.6 ± 26.6	166.7 ± 11.2
Stomach	248.9 ± 33.1	884.0 ± 619.8	353.2 ± 178.4	198.4 ± 18.2	257.0 ± 28.0	201.8 ± 16.3	152.0 ± 4.3	185.8 ± 26.2	249.4 ± 59.1	258.2 ± 38.2	227.9 ± 89.2	198.5 ± 9.3	197.4 ± 23.9	170.3 ± 11.7	189.8 ± 22.2	288.6 ± 55.5	166.5 ± 20.7
Intestine	270.2 ± 40.5	808.7 ± 473.3	237.2 ± 75.3	184.3 ± 19.5	261.3 ± 34.8	141.6 ± 2.1	141.4 ± 3.8	207.8 ± 28.9	192.6 ± 14.2	233.0 ± 19.8	194.4 ± 73.3	173.0 ± 9.5	166.7 ± 20.0	152.7 ± 12.1	289.4 ± 72.0	296.0 ± 36.8	168.3 ± 7.1
Muscle	197.6 ± 31.0	555.4 ± 320.9	213.5 ± 88.9	158.7 ± 21.6	185.3 ± 45.1	141.4 ± 5.1	134.2 ± 1.8	154.5 ± 15.0	171.6 ± 15.7	182.2 ± 8.1	180.6 ± 64.6	173.0 ± 6.1	184.6 ± 28.2	147.7 ± 7.4	188.8 ± 25.9	260.8 ± 14.3	147.0 ± 7.4
Brain	166.3 ± 10.8	253.5 ± 73.8	164.8 ± 30.8	147.7 ± 8.1	163.0 ± 24.3	136.8 ± 3.2	137.6 ± 2.9	147.8 ± 7.5	154.6 ± 6.7	159.0 ± 7.4	165.5 ± 30.7	157.8 ± 2.6	159.5 ± 17.9	146.7 ± 2.5	168.6 ± 14.0	214.2 ± 9.3	145.0 ± 6.9

The mean fluorescence values of each organ were normalized to the signal in kidney at 4 h (Table S2) for each mouse and then averaged for each variant; they are presented in Fig. S3. *n*, number of animals.

Table S4. Mean near infrared fluorescence with SD calculated for each organ collected at 4 and 24 h after Alexa750-K-pHLIP variant administration

Organ	K-Var3, 4 h $n = 11$	K-Var3, 24 h $n = 8$	K-Var7, 4 h $n = 10$	K-Var7, 24 h $n = 10$
Kidney	921.6 ± 306.2	254.5 ± 91.9	852.5 ± 345.0	235.2 ± 15.5
Tumor	395.9 ± 107.6	220.0 ± 70.0	306.0 ± 107.6	185.7 ± 9.8
Heart	319.6 ± 140.2	165.4 ± 51.1	228.2 ± 56.2	156.4 ± 27.7
Lungs	296.1 ± 66.9	154.1 ± 16.0	225.0 ± 80.0	136.2 ± 10.7
Liver	2,637.0 ± 6,446.4	684.2 ± 138.5	1,920.4 ± 752.3	538.2 ± 65.2
Spleen	1,057.5 ± 416.6	284.3 ± 32.0	552.3 ± 140.8	255.2 ± 80.1
Bladder	331.1 ± 100.1	176.5 ± 26.7	265.4 ± 70.9	155.3 ± 11.0
Stomach	286.2 ± 70.0	168.4 ± 20.2	260.6 ± 84.0	156.7 ± 15.5
Intestine	298.7 ± 46.0	173.9 ± 14.5	289.7 ± 84.9	166.9 ± 9.7
Muscle	201.3 ± 29.9	141.1 ± 15.6	178.8 ± 31.4	127.7 ± 4.2
Brain	192.5 ± 25.9	139.7 ± 5.9	158.8 ± 28.5	134.3 ± 2.9

n, number of animals.

Table S5. Mean near infrared fluorescence with SD calculated for each organ collected at 4 h after BODIPY-labeled Var3, K-Var3, Var7, and K-Var7 administration

Organ	Var3, 4 h $n = 4$	K-Var3, 4 h $n = 4$	Var7, 4 h $n = 4$	K-Var7, 4 h $n = 4$
Kidney	154.3 ± 14.4	128.8 ± 10.6	189.5 ± 51.0	121.3 ± 4.6
Tumor	325.0 ± 11.4	151.5 ± 16.7	308.0 ± 115.8	136.3 ± 9.3
Heart	128.3 ± 8.1	114.5 ± 6.0	124.0 ± 13.1	111.5 ± 3.5
Lungs	127.5 ± 11.4	116.0 ± 7.0	124.0 ± 11.6	111.0 ± 1.4
Liver	391.5 ± 78.9	152.8 ± 19.8	210.5 ± 67.6	142.3 ± 30.5
Spleen	122.0 ± 3.9	118.3 ± 4.5	125.0 ± 10.4	113.0 ± 4.2
Bladder	241.7 ± 23.8	150.8 ± 19.3	233.0 ± 64.6	143.8 ± 18.8
Stomach	257.0 ± 66.2	233.0 ± 75.2	269.8 ± 76.6	212.5 ± 26.6
Intestine	197.8 ± 26.7	159.0 ± 42.3	222.5 ± 118.3	133.0 ± 19.3
Muscle	150.5 ± 6.8	126.8 ± 3.0	141.0 ± 20.5	119.3 ± 4.8
Brain	142.0 ± 13.0	135.3 ± 11.8	131.5 ± 23.5	130.5 ± 7.9

n, number of animals.